Alterations in structure and mechanics of resistance arteries from ouabain-induced hypertensive rats

Ana M. Briones, Fabiano E. Xavier, Silvia M. Arribas, M. Carmen González, Luciana V. Rossoni, María J. Alonso and Mercedes Salaices

You might find this additional information useful...

This article cites 41 articles, 18 of which you can access free at:
http://ajpheart.physiology.org/cgi/content/full/291/1/H193#BIBL

Updated information and services including high-resolution figures, can be found at:
http://ajpheart.physiology.org/cgi/content/full/291/1/H193

Additional material and information about *AJP - Heart and Circulatory Physiology* can be found at:
http://www.the-aps.org/publications/ajpheart

This information is current as of February 19, 2007 .

Alterations in structure and mechanics of resistance arteries from ouabain-induced hypertensive rats

Ana M. Briones,[1] Fabiano E. Xavier,[1] Silvia M. Arribas,[2] M. Carmen González,[2] Luciana V. Rossoni,[3] María J. Alonso,[1,4] and Mercedes Salaices[1]

[1]*Departamento de Farmacología y Terapéutica and* [2]*Departamento de Fisiología, Facultad de Medicina, Universidad Autónoma de Madrid, Madrid, Spain;* [3]*Department of Physiology and Biophysics, Institute of Biomedical Sciences, University of Sao Paulo, SP, Brazil; and* [4]*Departamento de Ciencias de la Salud, Facultad de Ciencias de la Salud, Universidad Rey Juan Carlos, Alcorcón, Spain.*

Briones, Ana M., Fabiano E. Xavier, Silvia M. Arribas, M. Carmen González, Luciana V. Rossoni, María J. Alonso, and Mercedes Salaices. Alterations in structure and mechanics of resistance arteries from ouabain-induced hypertensive rats. *Am J Physiol Heart Circ Physiol* 291: H193–H201, 2006. First published February 10, 2006; doi:10.1152/ajpheart.00802.2005.—We have previously described that chronic administration of ouabain induces hypertension and functional alterations in mesenteric resistance arteries. The aim of this study was to analyze whether ouabain treatment also alters the structural and mechanical properties of mesenteric resistance arteries. Wistar rats were treated for 5 wk with ouabain (8.0 µg/day sc). The vascular structure and mechanics of the third-order branches of the mesenteric artery were assessed with pressure myography and confocal microscopy. Total collagen content was determined by picrosirius red staining, collagen I/III was analyzed by Western blot, and elastin was studied by confocal microscopy. Vascular reactivity was analyzed by wire myography. Internal and external diameters and cross-sectional area were diminished, whereas the wall-to-lumen ratio was increased in arteries from ouabain-treated rats compared with controls. In addition, arteries from ouabain-treated rats were stiffer. Ouabain treatment decreased smooth muscle cell number and increased total and I/III collagens in the vascular wall. However, this treatment did not modify adventitia and media thickness, nuclei morphology, elastin structure, and vascular reactivity to norepinephrine and acetylcholine. The present work shows hypotrophic inward remodeling of mesenteric resistance arteries from ouabain-treated rats that seems to be the consequence of a combination of decreased cell number and impaired distension of the artery, possibly due to a higher stiffness associated with collagen deposition. The narrowing of resistance arteries could play a role in the pathogenesis of hypertension in this model.

extracellular matrix; hypertension; arterial remodeling

SEVERAL FINDINGS suggest a putative role of endogenous ouabain-like compounds in the development and/or maintenance of hypertension (13, 36). Thus elevated circulating levels of endogenous ouabain have been demonstrated in humans with essential hypertension (15) as well as in several animal models of hypertension (14). In addition, exogenous ouabain and its structurally related analogs induce hypertension when chronically administered to normotensive rats (8, 16, 22, 24, 33, 39).

Hypertension induced by ouabain administration seems to depend, at least in part, on central mechanisms associated with increased sympathetic tone, subsequent to the activation of the brain renin-angiotensin (16, 40) and endothelin (8) systems. However, it is possible that additional peripheral mechanisms are also involved. Essential hypertension is associated with increased peripheral vascular resistance (27, 34). Its fundamental cause is a decrease in lumen diameter that could be originated by structural, mechanical, and/or functional alterations (6, 18). At peripheral level, ouabain-treatment alters vascular function in conductance and resistance arteries (22, 33, 39). However, whether this altered vascular reactivity is associated with structural changes of the resistance vasculature has never been explored.

The vascular structural alterations that accompany hypertension, known as "hypertensive arterial remodeling," are now considered to be a complex process that might involve the increase (hypertrophy), decrease (hypotrophy), or rearrangement (eutrophy) of wall material (26). The common feature is the decrease in internal diameter (inward remodeling). However, the contribution of growth to the structural abnormalities is different depending on the vascular bed and model of hypertension studied (18, 26). Thus small arteries from patients with essential hypertension show eutrophic remodeling (27), whereas mesenteric resistance arteries (MRA) and renal afferent arterioles from spontaneously hypertensive rats (SHR) show eutrophic and hypotrophic remodeling, respectively (5, 20, 29). However, secondary forms of human hypertension and experimental models with high circulating renin levels are characterized by inward hypertrophic remodeling (23, 32). A second common feature in hypertension is the alteration in the mechanical properties of resistance arteries. Thus arterial stiffness is increased in essential hypertensive patients and in some rat models of hypertension (18). Alterations in collagen, nonfibrous extracellular matrix proteins, adhesion molecules (18), and, more recently, in elastic fibers (5) have been proposed as determinants of the altered vascular stiffness and hypertensive arterial remodeling found in resistance arteries in hypertension.

The aim of the present study has been to test whether, in addition to the central mechanisms already described, alterations in the structure of resistance arteries might contribute to ouabain-induced hypertension. In particular, we have investigated *1*) gross structure and mechanics, *2*) cellular distribution,
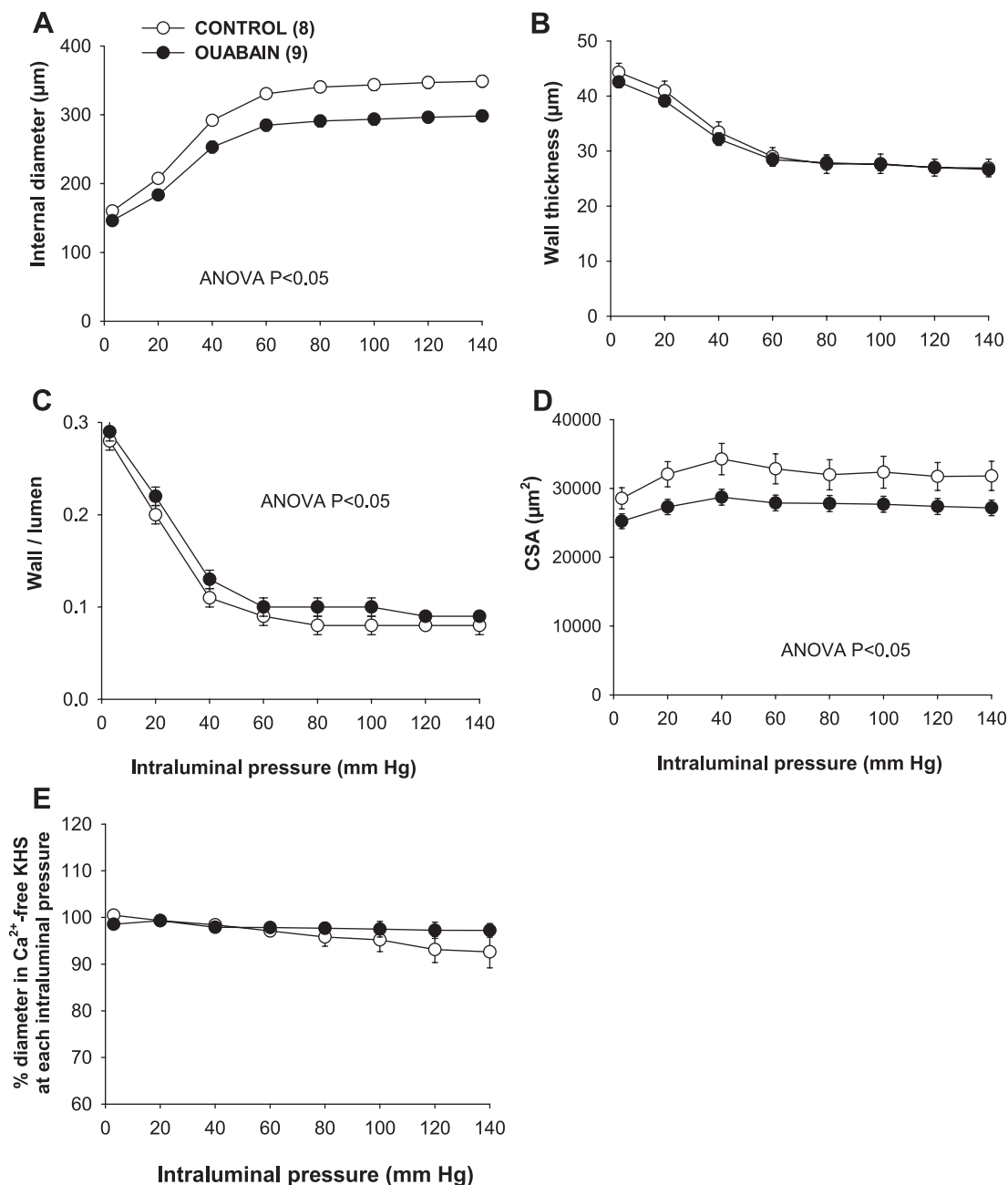
Fig. 1. Internal diameter-intraluminal pressure (*A*), wall thickness-intraluminal pressure (*B*), wall/lumen-intraluminal pressure (*C*), and cross-sectional area (CSA)-intraluminal pressure curves (*D*) in mesenteric resistance arteries from control and ouabain-treated rats incubated in calcium-free ($0Ca^{2+}$) Krebs-Henseleit solution (KHS). Pressure-induced myogenic responses in the presence of extracellular Ca^{2+} in arteries from the same rats is shown (*E*). Data are expressed as means ± SE. Number of animals in each case is indicated in parenthesis.

and *3*) content and distribution of fibrous extracellular matrix proteins in the vascular wall. To our knowledge, this is the first time that these parameters have been investigated in resistance arteries from this model of hypertension.

MATERIALS AND METHODS

Animal Model

Six-week-old male Wistar rats (Harlam Ibérica, Barcelona, Spain) were obtained from colonies maintained at the Animal Quarters of the Facultad de Medicina of the Universidad Autónoma de Madrid. Rats were housed at a constant room temperature, humidity, and light cycle (12:12-h light-dark) and had free access to tap water and standard rat chow ad libitum. The investigation conforms to the *Guide for the Care and Use of Laboratory Animals*, published by the National Institutes of Health (NIH Publication No. 85-23, Revised 1996) and the current Spanish and European laws (RD 223/88 MAPA and 609/86). The experimental protocol was approved by the Universidad Autónoma de Madrid Ethics Committee.

Rats were anesthetized with diethyl ether, and a small incision was made in the back of the neck to implant a subcutaneous controlled time-release pellet (Innovative Research of America, Sarasota, FL) containing ouabain (0.5 mg/pellet) or vehicle (placebo) as previously described (36). These pellets are designed to release a constant
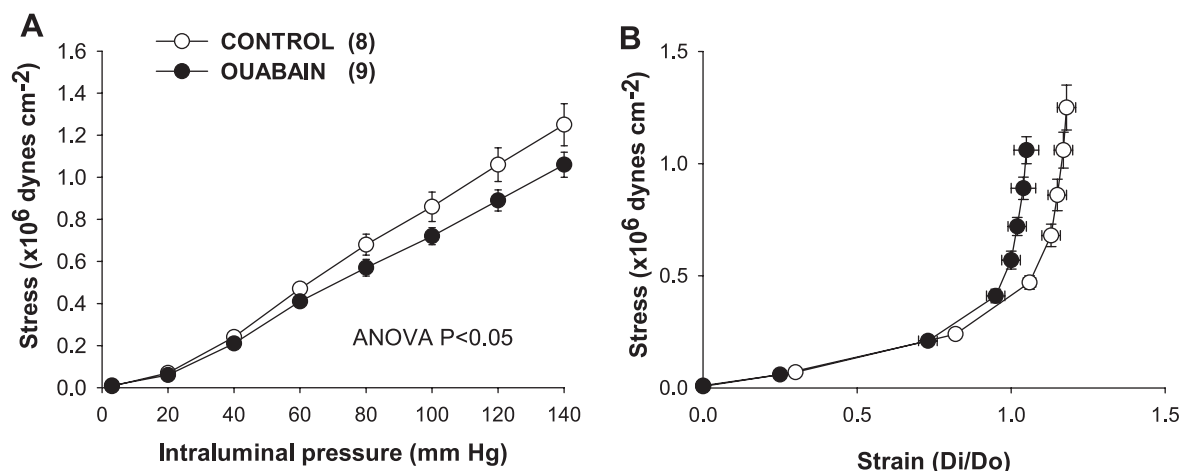
Fig. 2. Stress-intraluminal pressure (*A*) and stress-strain curves (*B*) in mesenteric resistance arteries from control and ouabain-treated rats incubated in $0Ca^{2+}$-KHS. Data are expressed as means ± SE. Number of animals in each case is indicated in parenthesis. D_o, internal diameter at 3 mmHg; D_i, observed internal diameter for a given intravascular pressure.

amount of either ouabain (≈8.0 µg/day) or vehicle for a 60-day period. The length of treatment was 5 wk. Systolic blood pressure (SBP) was measured by the tail-cuff method before the start of treatment and weekly during treatment.

The rats were decapitated, and the mesenteric arcade was removed and placed in Krebs-Henseleit solution (KHS) of the following composition (in mM): 115.0 NaCl, 4.7 KCl, 2.5 $CaCl_2$, 1.2 KH_2PO_4, 1.7 $MgSO_4 \cdot 7 H_2O$, 1.2 H_2O, 25.0 $NaHCO_3$, 11.1 glucose, and 0.01 Na_2EDTA. The mesenteric arcade was maintained at 4°C and continuously gassed with 95% O_2-5% CO_2. Third-order branches of the mesenteric arteries were isolated from the mesenteric bed and carefully cleaned of surrounding tissue under a dissecting microscope.

Pressure Myography

The structural and mechanical properties of MRAs were studied with a pressure myograph (Danish Myo Tech, model P100, J. P. Trading, Aarhus, Denmark), as previously described (5). Briefly, the artery was placed on two glass microcannulae and secured with surgical nylon suture. After any small branches were tied off, artery length was adjusted so that the artery walls were parallel without stretch. Intraluminal pressure was then raised to 140 mmHg, and the artery was unbuckled by adjusting the cannulae. The segment was set to a pressure of 70 mmHg and allowed to equilibrate for 30 min at 37°C in KHS gassed with a mixture of 95% O_2-5% CO_2. Intraluminal

pressure was then reduced to 3 mmHg, and a pressure-diameter curve was obtained by increasing intraluminal pressure in 20-mmHg steps between 3 and 140 mmHg. Internal and external diameters (D_i and D_e) were measured for 3 min at each intraluminal pressure. Thereafter, the segment was perfused with calcium-free ($0Ca^{2+}$) KHS (by omitting calcium and adding 10 mM EGTA) for 30 min. A second pressure-diameter curve was obtained, and internal and external diameters were measured under passive conditions (D_{i0Ca} and D_{e0Ca}). Finally, the artery was set to 70 mmHg in $0Ca^{2+}$-KHS, pressure fixed with 4% paraformaldehyde (PFA, in 0.2 M phosphate buffer, pH 7.2–7.4) at 37°C for 60 min and kept in 4% PFA at 4°C for confocal microscopy.

Pressure-induced myogenic responses. The myogenic index (MI) was calculated as follows (12):

$$MI = (100 \times \Delta D_i/D_o)/\Delta IP,$$

where D_i is the internal diameter at any given pressure, D_o is the diameter at the previous intraluminal pressure, and ΔIP is the change in intraluminal pressure (ΔIP were made in 20-mmHg steps).

To quantify the active vasoconstriction of the arteries for each intraluminal pressure, some results were expressed as a percentage of the diameter of each artery under passive conditions at each intraluminal pressure.

Calculation of passive structural and mechanical parameters. From internal and external diameter measurements in passive conditions, the following structural parameters were calculated: wall thickness = $(D_{e0Ca} - D_{i0Ca})/2$; cross-sectional area (CSA) = $(\pi/4) \times (D_{e0Ca}^2 - D_{i0Ca}^2)$; and wall/lumen = $(D_{e0Ca} - D_{i0Ca})/2D_{i0Ca}$.

The following mechanical parameters were calculated according to the method of Baumbach and Heistad (3): circumferential wall strain (ε) = $(D_{i0Ca} - D_{00Ca})/D_{00Ca}$, where D_{00Ca} is the internal diameter at 3 mmHg and D_{i0Ca} is the observed internal diameter for a given intravascular pressure both measured in $0Ca^{2+}$ medium; and circumferential wall stress (σ) = $(P \times D_{i0Ca})/(2WT)$, where P is the intraluminal pressure (1 mmHg = 133.4 N/m^2) and WT is wall thickness at each intraluminal pressure in $0Ca^{2+}$ medium.

Arterial stiffness independent of geometry is determined by Young's elastic modulus (E = stress/strain). The stress-strain relationship is nonlinear; therefore, it is more appropriate to obtain a tangential or incremental elastic modulus (E_{inc}) by determining the slope of the stress-strain curve ($E_{inc} = \delta\sigma/\delta\varepsilon$) (10). E_{inc} was obtained by fitting the stress-strain data from each animal to an exponential curve by using the equation

$$\sigma = \sigma_{orig}e^{\beta\varepsilon}$$

where σ_{orig} is the stress at the original diameter (diameter at 3

Table 1. *Laser scanning confocal microscope measurements of mesenteric resistance artery morphology in control and ouabain-treated rats*

	Control	Ouabain
n	8	8
Adventitia thickness, µm	6.5±0.3	5.9±0.5
Media thickness, µm	11.1±0.6	11.6±0.9
LSA, mm²	1.02±0.03	0.91±0.03*
Wall volume, mm³	0.034±0.001	0.029±0.002*
Total number of cells		
(AC + SMC + EC)	7,381±272	6,407±345*
Total number of AC	1,421±58	1,269±109
Total number of SMC	4,515±220	3,859±201*
Total number of EC	1,445±37	1,279±110

Values are means ± SE; *n*, no. of animals. All calculations were performed on the basis of 1-mm-long segments. LSA, luminal surface area; AC, adventitial cells; SMC, smooth muscle cells; EC, endothelial cells. *$P < 0.05$ with respect to control rats.
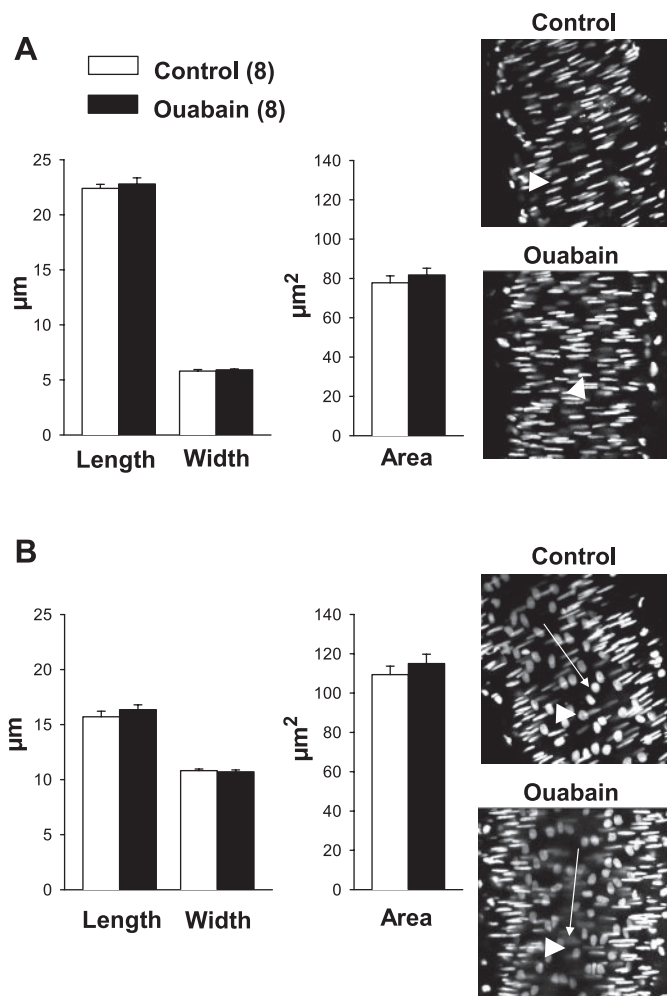
Fig. 3. *Left*: comparison of morphological parameters of smooth muscle (SMC; *A*) and endothelial cell (EC; *B*) nuclei from images of pressure-fixed mesenteric resistance arteries from control and ouabain-treated rats. *Right*: representative microphotographs of laser scanning confocal microscopy images of SMC (*A*) and EC (*B*) nuclei from mesenteric resistance arteries from control and ouabain-treated rats. Arteries were incubated with 0.01 mg/ml Hoechst 33342 to stain cell nuclei. Images were taken from slide-mounted vessels with an ×63 oil objective, ×1 zoom with a laser scanning confocal microscope. Lines with arrows show longitudinal axis of vessel. Arrowheads point to representative nuclei. Image dimensions are 238 × 238 μm. Number of animals in each case is indicated in parenthesis.

mmHg). Taking derivatives on the above equation, we see that $E_{\text{inc}} = \beta\sigma$. For a given σ value, E_{inc} is directly proportional to β. An increase in β implies an increase in E_{inc}, which means an increase in stiffness.

Confocal Microscopy

Confocal microscopy study of nuclei distribution. Pressure-fixed intact arteries were incubated with the nuclear dye Hoechst 33342 (0.01 mg/ml) for 15 min. After being washed, arteries were mounted on slides with a well made of silicon spacers to avoid artery deformation. They were viewed with a Leica TCS SP2 confocal system fitted with an inverted microscope and argon and helium-neon laser sources with oil immersion lens (×63) (excitation wavelength 351–364 nm and emission wavelength 400–500 nm). Two stacks of images of 0.5-μm-thick serial optical slices were taken from the adventitia to the lumen in different regions along the artery length. Individual images of the endothelial layer were also captured. Meta-Morph Image Analysis Software (Universal Imaging) was used for

quantification. The adventitia and the media thickness and nuclei number were measured in the *z*-axis, as previously described (2). To allow a comparison of control and ouabain-treated rats, the following calculations were performed on the basis of 1-mm-long segments: *1*) artery volume (in mm^3) [volume = wall CSA (in mm^2) × 1 mm]; *2*) total number of adventitial and smooth muscle cells (SMC) (cell number = the number of nuclei per stack times the number of stacks per artery volume); and *3*) the total number of endothelial cells per luminal surface of a 1-mm-long artery (luminal surface area = $2\pi D/2$).

Confocal microscopy study of elastin content and organization. The content and organization of elastin were studied in MRA with fluorescent confocal microscopy based on the autofluorescent properties of elastin (excitation wavelength 488 nm and emission wavelength 500–560 nm) (38). The experiments were performed in intact pressure-fixed MRA with a Leica TCS SP2 confocal system. Serial optical sections from the adventitia to the lumen (z step= 0.3 μm) were captured with a ×63 oil objective (numerical aperture 1.3) using the 488-nm line of the confocal microscope. A minimum of two stacks of images of different regions was captured in each arterial segment. All the images were taken under identical conditions of laser intensity, brightness, and contrast.

Quantitative analysis was performed with MetaMorph Image Analysis Software, as previously described (5). From each stack of serial images, individual projections of the internal elastic lamina (IEL) were reconstructed, and IEL thickness, total fenestrae number, fenestra area, and relative area occupied by elastin were measured. Fluorescent intensity values were used as an estimate of the elastin concentration as previously described (5), based on the assumption that the concentration of elastin has a linear relationship with fluorescence intensity (4).

Collagen Determination by Picrosirius Red

In a separate set of experiments, segments of MRA were removed from the mesentery and immediately fixed in 4% PFA in phosphate buffer for 1 h, transferred to a cryomold containing optimum cutting temperature embedding medium (Tissue Tek, Sakura), and frozen in liquid nitrogen. Frozen transverse sections (10 μm) were incubated with picrosirius red [0.1% (wt/vol) Sirius red 3FB in saturated aqueous picric acid] for 30 min with gentle agitation for collagen staining (21). Color images were captured with a microscope (Nikon Eclipse TE 2000-S, ×40 objective) by using a digital camera (Nikon DXM 1200F). Quantitative and qualitative analyses of collagen content and distribution were performed with MetaMorph Image Analysis Software (Universal Imaging). Original images were transformed to grayscale level. Thereafter, collagen content was estimated separately in the adventitial and medial layers by subtracting the background from the intensity values obtained in the medial or adventitial area of each cross section. In addition, grayscale images from control and ouabain-treated rats were thresholded at the same level, and images showing the distribution of collagen in the vascular wall were obtained.

Western Blot Analysis

Collagen I/III protein expression was determined in homogenates (50 μg protein) from MRA of control and ouabain-treated rats. Proteins were separated by 7.5% SDS-PAGE and then transferred to nitrocellulose membranes for 1.5 h. Membranes were incubated with rabbit polyclonal antibody for collagen I/III (1:500 dilution; Calbiochem, San Diego, CA) and mouse monoclonal antibody for α-actin (1:10,000, Sigma Chemical, St. Louis, MO). After being washed, membranes were incubated with anti-rabbit (1:2,000) or anti-mouse (1:10,000) IgG antibodies conjugated to horseradish peroxidase (Bio-Rad, Hercules, CA). The immunocomplexes were detected with the use of an enhanced horseradish peroxidase-luminol chemiluminescence system (ECL Plus; Amersham International, Little Chalfont,
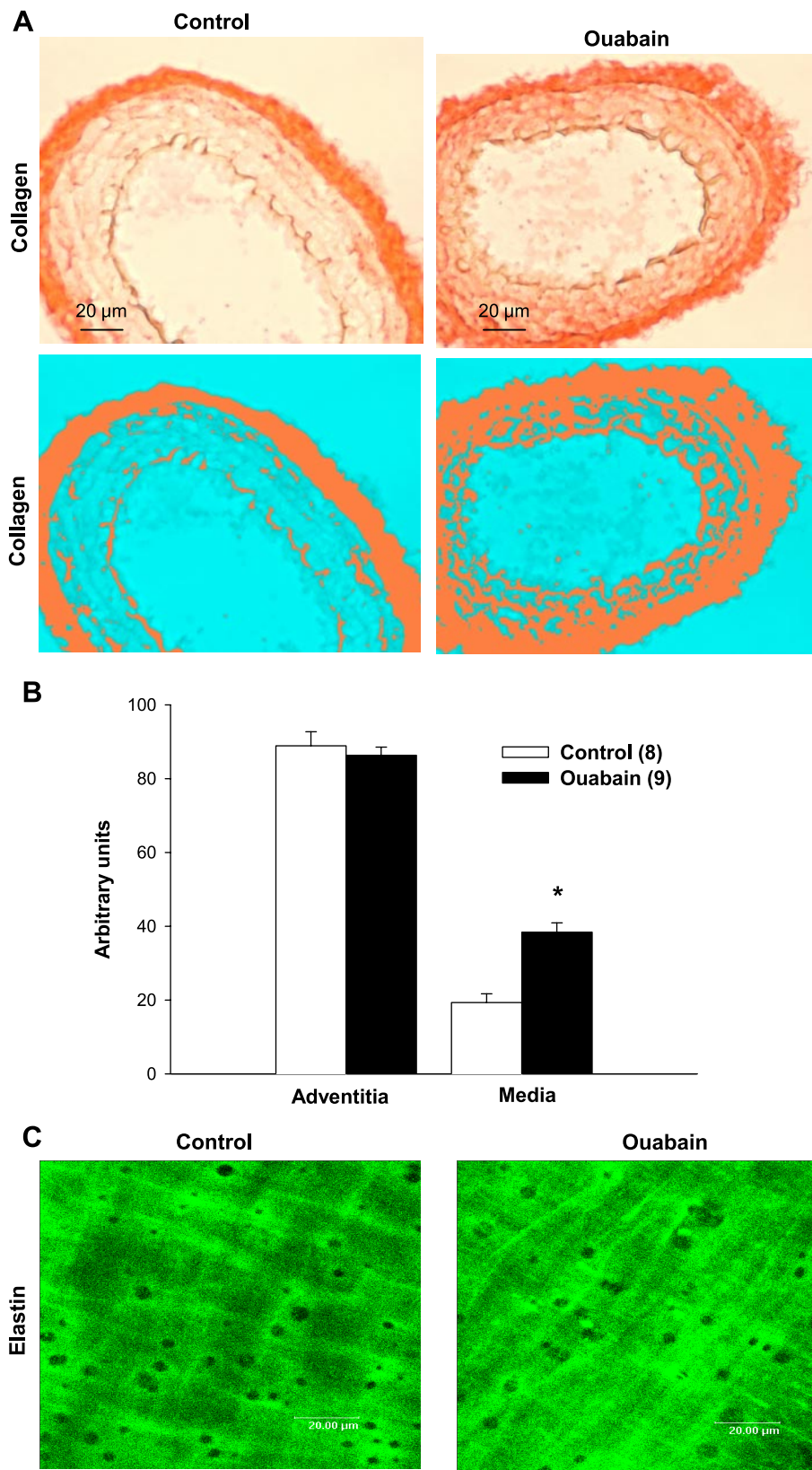
A

B

C

Fig. 4. *A*: representative images of collagen staining with picrosirius red of transversal sections obtained from mesenteric resistance arteries from control and ouabain-treated rats. *A*, *top*: original images. *A*, *bottom*: same images after thresholding. Images were captured with a light microscope (×40 objective, ×1 zoom). *B*: quantitative analysis of collagen content in adventitia and media. *P < 0.05 vs. control. *C*: confocal projections of the internal elastic lamina of mesenteric resistance arteries from control and ouabain-treated rats. Vessels were pressure-fixed at 70 mmHg and mounted intact on a slide. Projections were obtained from serial optical sections captured with a fluorescence confocal microscope (×63 oil immersion objective, ×2 zoom). Data are expressed as means ± SE. Number of animals in each case is indicated in parenthesis.
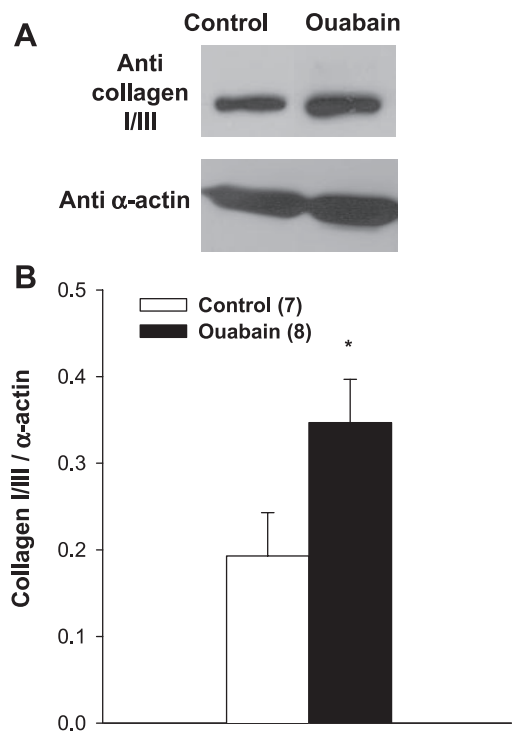
A

B

Fig. 5. Representative blot (*A*) and densitometric analysis of collagen I/III protein expression (*B*) in mesenteric resistance arteries from control and ouabain-treated rats. Expression of α-actin, as a loading control, is also shown. Results are means ± SE. Number of animals in each case is indicated in parenthesis. *$P < 0.05$.

UK) and subjected to autoradiography (Hyperfilm ECL, Amersham International). Signals on the immunoblot were quantified with the NIH Image computer program (version 1.56).

Protein expression data are expressed as the ratio between signals on the immunoblot corresponding to collagen I/III and α-actin.

Vascular Reactivity Experiments

With the use of a dissecting microscope, third-order MRAs were isolated, divided into segments ~2 mm in length, and mounted in a small vessel dual chamber myograph for measurement of isometric tension according to the method described by Mulvany and Halpern (25). After a 45-min equilibration period in oxygenated KHS at 37°C, pH 7.4, MRA were exposed to 120 mM KCl to check their functional integrity. Then, concentration-response curves to ACh (0.01 nM-30 μM) were performed in arteries submaximally contracted with norepinephrine at a concentration that produced ~50% of the contraction induced by KCl. After a washout period of 60 min, concentration-response curves to norepinephrine (10 nM-30 μM) were performed in the same arteries. At the end of all experiments, segments were thoroughly washed, and KHS was replaced by 120 mM K⁺-KHS; once the contraction was stable, 0.1 mM papaverine was added. Vascular responses were calculated as active wall tension (increase in vessel force above resting level divided by twice the arterial segment length). The maximum response of the arteries [2.9 ± 0.2 and 3.1 ± 0.1 mN/mm for control ($n = 11$) and ouabain ($n = 14$)-treated rats, respectively] was determined by the difference between the tone generated by the first 120 mM K⁺-KHS and that produced by papaverine. Contraction to norepinephrine was expressed as a percentage of the maximum response of the arteries. Relaxation induced by ACh was expressed as a percentage of the tone previously obtained with norepinephrine.

Results are expressed as means ± SE, and *n* denotes the number of animals used in each experiment. The dependency of either vascular structure or mechanics on rat treatment group and intraluminal pressure was studied by two-way ANOVA. For specific two-means comparison, an unpaired Student's *t*-test was used. A value of $P < 0.05$ was considered significant.

Norepinephrine, ACh, papaverine, Hoechst 33342, and Sirius red were obtained from Sigma-Aldrich. All other chemicals were of reagent grade or better and obtained from Sigma Chemical or other commercial suppliers.

RESULTS

Ouabain treatment progressively increased SBP from the first week of treatment, as previously described by our group (31, 36). At the end of the treatment, control and ouabain-treated rats showed the following SBP values: control, 118 ± 1.5 ($n = 8$); ouabain, 149 ± 2.0 mmHg ($n = 9$) ($P < 0.05$). The body weight was similar in both experimental groups [control, 327 ± 10 ($n = 8$); ouabain, 339 ± 17 g ($n = 9$)].

Vascular Structure and Mechanics

Figure 1 shows the structural parameters of MRA from control and ouabain-treated rats under fully relaxed conditions ($0Ca^{2+}$-KHS). Internal diameter (Fig. 1*A*) and external diameter (data not shown) were diminished in arteries from ouabain-treated rats compared with controls. However, wall thickness was similar in both groups at all pressures studied (Fig. 1*B*). As a consequence, wall-to-lumen ratio was higher and CSA was smaller in MRA from ouabain-treated rats compared with controls (Fig. 1, *C* and *D*).

In active conditions, i.e, in the presence of extracellular calcium, external and internal diameters were also significantly reduced in ouabain-treated rats compared with controls (data not shown). MRA had a small level of myogenic tone at all pressures tested that was similar in both groups (data not shown). Similarly, there was no statistical difference in intrinsic tone between control and ouabain-treated rats (Fig. 1*E*).

Figure 2 shows the mechanical parameters of MRA from control and ouabain-treated rats. Media stress was significantly smaller in arteries from ouabain-treated rats than in control animals (Fig. 2*A*). In addition, MRA from ouabain-treated rats showed decreased elasticity, as shown by the larger value of β [control, 4.17 ± 0.07 ($n = 8$); ouabain, 4.67 ± 0.14 ($P < 0.05$; $n = 9$)] and a leftward shift of the stress-strain relationship (Fig. 2*B*).

Table 2. *Characteristics of IEL in pressurized segments of mesenteric resistance arteries from control and ouabain-treated rats*

	Control	Ouabain
n	7	9
IEL thickness, μm	3.5±0.1	3.5±0.1
Total number of fenestrae	3,437±409	3,265±428
Fenestra area, μm²	13.8±1.3	12.7±0.9
Relative area of elastin/image	0.80±0.01	0.79±0.01
Intensity/pixel	113.80±1.32	116.90±1.52
Total fluorescence (×10⁶), intensity·pixel⁻¹·vol⁻¹	4,085±195	3,658±131

Values are means ± SE; *n*, no. of animals. IEL, internal elastic lamina.

Morphology of Vascular Wall

Adventitia and media thickness were similar in control and ouabain-treated rats (Table 1). As expected, luminal surface area and wall volume were significantly smaller in arteries from ouabain-treated rats (Table 1). The total number of cells (adventitial plus smooth muscle plus endothelial cells) was diminished in ouabain-treated rats compared with control rats. When each cell type was analyzed separately, only the SMC number was statistically different (Table 1).

Results of smooth muscle and endothelial cells nuclei morphology are shown in Fig. 3. There was no difference in either the length or width of cell nuclei between both groups. Consequently, nuclei area was similar in control and ouabain-treated rats (Fig. 3).

Collagen and Elastin Quantification

As shown in Fig. 4*A*, collagen was present throughout the whole vascular wall, being more densely distributed in the adventitia. Ouabain treatment did not affect collagen content in the adventitia. However, ouabain treatment significantly increased collagen content in the media (Fig. 4*B*). Western blot experiments showed increased collagen I/III expression in MRA from ouabain-treated rats compared with controls (Fig. 5).

Figure 4*C* shows maximal intensity projections of the IEL from control and ouabain-treated rats, and Table 2 resumes the quantification of the IEL characteristics. We did not find any differences in the structure of elastin in the IEL between arteries from normotensive and hypertensive rats, because both fenestrae area and number were similar. Average fluorescence intensity per pixel was not significantly different between control and ouabain-treated rats, indicating no evidence for a difference in the total amount of elastin in a 1-mm length of artery.

Vascular Reactivity

KCl (120 mM) evoked similar contractions in vessels from ouabain-treated and control rats [control, 9.4 ± 0.7 ($n = 11$); ouabain-treated, 9.3 ± 0.6 mN ($n = 14$)]. The endothelium-dependent relaxation to ACh and contractile responses to norepinephrine also remained unchanged after ouabain treatment (Fig. 6).

DISCUSSION

Elevated levels of endogenous ouabain or a closely related isomer are implicated in rat and human hypertension and in associated cardiovascular complications. Thus, in $\sim$30% of patients with uncomplicated essential hypertension, plasma endogenous ouabain levels are increased. Several findings indicate that endogenous ouabain, in addition to directly influencing blood pressure, may be involved in the development of cardiovascular complications (cardiac hypertrophy, heart failure, and myocardial infarction) associated with hypertension. Endogenous ouabain may therefore play a direct role in vivo as a prohypertrophic hormone and thus may affect cardiovascular function and structure, being responsible for cardiac remodeling that contributes to an increased risk of morbid events (13, 14, 15, 36). Furthermore, exogenous ouabain induces hypertension when chronically administered to normotensive rats (24, 39). Central and peripheral mechanisms have been suggested as possible participants in the hypertension induced by ouabain (33, 39, 40). However, the contribution of structural alterations of resistance arteries to this model of hypertension has not been analyzed so far.

Hypertension is characterized by increased peripheral vascular resistance to blood flow. According to Poiseuille's law, flow resistance is inversely related to the fourth power of the vessel's radius. Therefore, small decreases in the lumen of small arteries and arterioles will significantly increase resistance (27, 35). We observed that MRA from ouabain-treated rats showed decreased internal and external diameters in active conditions. At the functional level, both an increase in the contractile responses or a decrease in relaxant responses might increase peripheral resistance by reducing internal diameter. However, our experimental data seem to exclude functional changes as responsible for the observed decrease in vessel size in this model of hypertension. This is based on three observations: *1*) no difference between treatment groups in either MI or intrinsic tone; *2*) unaltered vasoconstrictor responses to K^+ or norepinephrine; and *3*) unaltered ACh-induced relaxation. Moreover, we have previously reported that the modulation of norepinephrine responses by endothelial nitric oxide was higher in ouabain-treated rats compared with controls (39).

Structural and mechanical changes in resistance arteries may result in decreased lumen size (35). In passive conditions, we
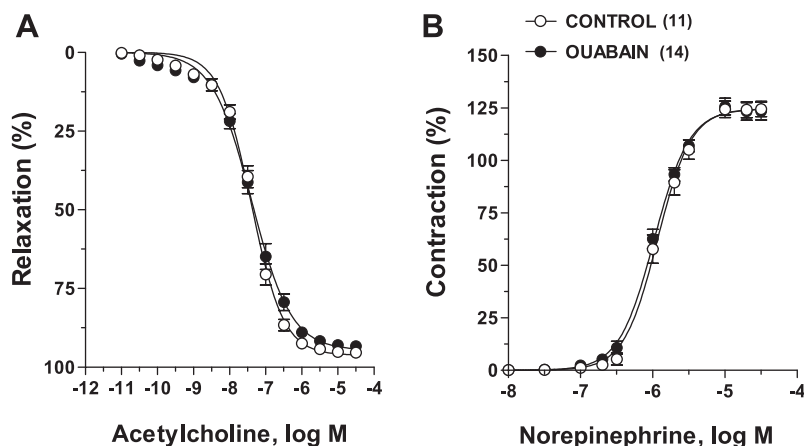
Fig. 6. Endothelium-dependent vasodilator responses to acetylcholine (*A*) and contractile responses to norepinephrine (*B*) of mesenteric resistance arteries from control and ouabain-treated rats. Data are expressed as means $\pm$ SE. Number of animals in each case is indicated in parenthesis.

also observed decreased internal and external diameters in MRA from ouabain-treated rats. In other models of hypertension, the reduction in internal diameter is associated with thickening of the vessel wall (6, 18, 27); in our experimental model, wall thickness remained unchanged. However, we observed diminished CSA. This alteration, together with decreased vessel diameter, is a typical feature of hypotrophic inward remodeling (26), which has been previously described in afferent arterioles from SHR (29). Mechanisms underlying hypotrophic remodeling are unclear. Atrophy of one or more layers of the vascular wall due to decreased cellular number might be implicated in the development of hypotrophic arterial remodeling. In this sense, Coats et al. (7) reported atrophy in both the medial and adventitial layers of the artery wall of distal ischemic arteries due to hypoplasia. We found a decrease in the total number of cells, mainly due to decreased SMC number, in arteries from ouabain-treated rats. Thus some signs of hypoplasia seem to appear after ouabain treatment. In this line, Orlov et al. (31) recently reported that long-term exposure to ouabain culminates in porcine aortic endothelial cell necrosis mediated by the interaction of ouabain with Na^+-K^+-ATPase. Another possibility to explain hypotrophic arterial remodeling could be a decrease in cell size. Because we and other authors have demonstrated changes in the morphology of endothelial or SMC nuclei in other models of hypertension (1, 2, 9) and there is evidence that SMC nuclear size correlates with SMC length (9), we analyzed possible changes in endothelial cells and SMC nuclei morphology. However, the size of nuclei from both cell types was not modified by ouabain treatment, pointing to the reduction in cell number as responsible for hypotrophic remodeling observed in ouabain-treated rats.

The decrease in internal diameter could be originated by a structural modification, i.e., "true hypertensive remodeling" or by a mechanical alteration of the vessels (6, 18). We observed increased stiffness in MRA from ouabain-treated rats as shown by the leftward shift of the stress-strain relationship and the increased β value (which reflects arterial stiffness independent of vessel geometry). Stiffness is increased in MRA from SHR (5, 20), whereas no differences in intrinsic elastic properties were found in MRA from other models of hypertension, such as Dahl salt-sensitive (17) and mRen-2 transgenic rats (11). In resistance arteries, enhanced vascular stiffness in hypertension has been generally attributed to an increase in collagen content (19, 20, 37), nonfibrous extracellular matrix proteins and adhesion molecules (18), and, more recently, to changes in elastic fiber organization of the IEL (5). Arteries from ouabain-treated rats showed increased collagen deposition in the media but not in the adventitia. Fibrillar type I/III collagens are the most abundant in the vascular wall (28), and they play an important role controlling arterial expansion (10). Therefore, we explored expression of these types of collagens. Our results show augmented expression of type I/III collagens in arteries from ouabain-treated rats, suggesting increased synthesis as the mechanism responsible of the increased collagen deposition. In our experimental model, we did not observe differences in either the organization of the IEL or in elastin fluorescence, which provides an estimate of the elastin concentration (4). Our results, therefore, point to an increase in collagen deposition as responsible for the changes in vascular mechanics and, possibly, in inward remodeling in this model of hypertension.

In summary, the present work demonstrates hypotrophic inward remodeling of MRA from ouabain-treated rats that seems to be the consequence of a combination of decreased cell number and impaired distension of the vessel, possibly due to a higher stiffness associated with collagen deposition. We suggest that the narrowing of resistance vessels could play a role in the pathogenesis of hypertension in this model. There are several reports analyzing, in different cultured cell types, the effect of sustained inhibition of the Na^+-K^+ pump in macromolecular synthesis and cell proliferation (30, 31). The present experimental model seems to represent a good experimental approach to look into the geometry of resistance arteries after administration of ouabain. However, to assess the role of endogenous ouabain in hypertensive vascular remodeling, it would be useful to study the effect of antibodies against endogenous Na^+-K^+ pump inhibitors in other experimental models of hypertension. Another possibility would be the use of the ouabain antagonist PST 2238, a new antihypertensive compound that selectively antagonizes the pressor effect and the alteration of the renal Na-K pump and ouabain-induced organ hypertrophy (13).

REFERENCES

1. **Arribas SM, González C, Graham D, Dominiczak AF, and McGrath JC.** Cellular changes induced by chronic nitric oxide inhibition in intact rat basilar arteries revealed by confocal microscopy. *J Hypertens* 15: 1685–1693, 1997.
2. **Arribas SM, Hillier C, González C, McGrory S, Dominiczak AF, and McGrath JC.** Cellular aspects of vascular remodeling in hypertension revealed by confocal microscopy. *Hypertension* 30: 1455–1464, 1997.
3. **Baumbach GL and Heistad DD.** Remodeling of cerebral arterioles in chronic hypertension. *Hypertension* 13: 968–792, 1989.
4. **Blomfield J and Farrar JF.** The fluorescent properties of maturing arterial elastin. *Cardiovasc Res* 3: 161–170, 1969.
5. **Briones AM, González JM, Somoza B, Giraldo J, Daly CJ, Vila E, González MC, McGrath JC, and Arribas SM.** Role of elastin in spontaneously hypertensive rat small mesenteric artery remodelling. *J Physiol* 552: 185–195, 2003.
6. **Bund SJ and Lee RM.** Arterial structural changes in hypertension: a consideration of methodology, terminology and functional consequence. *J Vasc Res* 40: 547–557, 2003.
7. **Coats P, Jarajapu YPR, Hillier C, McGrath JC, and Daly C.** The use of fluorescent nuclear dyes and laser scanning confocal microscopy to study the cellular aspects of arterial remodelling in human subjects with critical limb ischaemia. *Exp Physiol* 88: 547–554, 2003.
8. **Di Filippo C, Filippelli A, Rinaldi B, Piegari E, Esposito F, Rossi F, and D'Amico M.** Chronic peripheral ouabain treatment affects the brain endothelin system of rats. *J Hypertens* 21: 747–753, 2003.
9. **Dickhout JG and Lee RMKW.** Increased medial smooth muscle cell length is responsible for vascular hypertrophy in young hypertensive rats. *Am J Physiol Heart Circ Physiol* 279: H2085–H2094, 2000.
10. **Dobrin PB.** Mechanical properties of arteries. *Physiol Rev* 58: 397–460, 1978.
11. **Dunn WR and Gardiner SM.** Differential alteration in vascular structure of resistance arteries isolated from the cerebral and mesenteric vascular

beds of transgenic [(mRen-2)27], hypertensive rats. *Hypertension* 29: 1140–1147, 1997.

12. **Dunn WR, Wallis SJ, and Gardiner SM.** Remodelling and enhanced myogenic tone in cerebral resistance arteries isolated from genetically hypertensive Brattleboro rats. *J Vasc Res* 35: 18–26, 1998.

13. **Ferrandi M, Manunta P, Ferrari P, and Bianchi G.** The endogenous ouabain: molecular basis of its role in hypertension and cardiovascular complications. *Front Biosci* 10: 2472–2477, 2005.

14. **Hamlyn JM, Hamilton BP, and Manunta P.** Endogenous ouabain, sodium balance and blood pressure: a review and a hypothesis. *J Hypertens* 14: 151–171, 1996.

15. **Hamlyn JM, Ringel R, Schaeffer J, Levinson PD, Hamilton BP, Kowearski AA, and Blaustein MP.** A circulating inhibitor of (Na^+, K^+) ATPase is associated with essential hypertension. *Nature* 300: 650–652, 1982.

16. **Huang BS and Leenen FHH.** Brain renin-angiotensin system and ouabain-induced sympathetic hyperactivity and hypertension in Wistar rats. *Hypertension* 34: 107–112, 1999.

17. **Intengan HD and Schiffrin EL.** Mechanical properties of mesenteric resistance arteries from Dahl salt-resistant and salt-sensitive rats: role of endothelin-1. *J Hypertens* 16: 1907–1912, 1998.

18. **Intengan HD and Schiffrin EL.** Structure and mechanical properties of resistance arteries in hypertension. Role of adhesion molecules and extracellular matrix determinants. *Hypertension* 36: 312–318, 2000.

19. **Intengan HD, Deng LY, Li JS, and Schiffrin EL.** Mechanics and composition of human subcutaneous resistance arteries in essential hypertension. *Hypertension* 33: 569–574, 1999.

20. **Intengan HD, Thibault G, Li JS, and Schiffrin EL.** Resistance artery mechanics, structure, and extracellular components in spontaneously hypertensive rats. Effects of angiotensin receptor antagonism and converting enzyme inhibition. *Circulation* 100: 2267–2275, 1999.

21. **Izzard AS, Graham D, Burnham MP, Heerkens EH, Dominiczak AF, and Heagerty AM.** Myogenic and structural properties of cerebral arteries from the stroke-prone spontaneously hypertensive rat. *Am J Physiol Heart Circ Physiol* 285: H1489–H1494, 2003.

22. **Kimura K, Manunta P, Hamilton BP, and Hamlyn JM.** Different effects of in vivo ouabain and digoxin on renal artery function and blood pressure in the rat. *Hypertens Res* 23: S67–S76, 2000.

23. **Korsgaard N and Mulvany MJ.** Cellular hypertrophy in mesenteric resistance vessels from renal hypertensive rats. *Hypertension* 12: 162–167, 1988.

24. **Manunta P, Rogowski AC, Hamilton BP, and Hamlyn JM.** Ouabain-induced hypertension in the rat: relationships among plasma and tissue ouabain and blood pressure. *J Hypertens* 12: 549–560, 1994.

25. **Mulvany MJ and Halpern W.** Contractile properties of small arterial resistance vessels in spontaneously hypertensive and normotensive rats. *Circ Res* 41: 19–26, 1977.

26. **Mulvany MJ, Baumbach GL, Aalkjaer C, Heagerty AM, Korsgaard N, Schiffrin EL, and Heistad DD.** Vascular remodeling. *Hypertension* 28: 505–506, 1996.

27. **Mulvany MJ.** Small artery remodeling and significance in the development of hypertension. *News Physiol Sci* 17: 105–109, 2002.

28. **Murata K, Motayama T, and Kotake C.** Collagen types in various layers of the human aorta and their changes with the atherosclerotic process. *Atherosclerosis* 60: 251–262, 1986.

29. **Norrelund H, Christensen KL, Samani NJ, Kimber P, Mulvany MJ, and Korsgaard N.** Early narrowed afferent arteriole is a contributor to the development of hypertension. *Hypertension* 24: 301–308, 1994.

30. **Orlov SN, Taurin S, Tremblay J, and Hamet P.** Inhibition of Na^+, K^+ pump affects nucleic acid synthesis and smooth muscle cell proliferation via elevation of the $[Na^+]_i/[K^+]_i$ ratio: possible implication in vascular remodelling. *J Hypertens* 19: 1559–1565, 2001.

31. **Orlov SN, Thorin-Trescases N, Pchejetski D, Taurin S, Farhat N, Tremblay J, Thorin E, and Hamet P.** Na^+/K^+ pump and endothelial cell survival: $[Na^+]_i/[K^+]_i$-independent necrosis triggered by ouabain, and protection against apoptosis mediated by elevation of $[Na^+]_i$. *Pflügers Arch* 448: 335–345, 2004.

32. **Rizzoni D, Porteri E, Guefi D, Piccoli A, Castellano M, Pasini G, Muiesan ML, Mulvany MJ, and Rosei EA.** Cellular hypertrophy in subcutaneous small arteries of patients with renovascular hypertension. *Hypertension* 35: 931–935, 2000.

33. **Rossoni LV, Salaices M, Marín J, Vassallo DV, and Alonso MJ.** Alterations on vascular reactivity to phenylephrine and Na^+, K^+-ATPase activity and expression in hypertension induced by chronic administration of ouabain. *Br J Pharmacol* 135: 771–781, 2002.

34. **Schiffrin EL and Touyz RM.** From bedside to bench to bedside: role of renin-angiotensin-aldosterone system in remodeling of resistance arteries in hypertension. *Am J Physiol Heart Circ Physiol* 287: H435–H446, 2004.

35. **Schiffrin EL.** Remodeling of resistance arteries in essential hypertension and effects of antihypertensive treatment. *Am J Hypertens* 17: 1192–1200, 2004.

36. **Schoner W and Scheiner-Bobis G.** Endogenous cardiac glycosides: hormones using the sodium pump as signal transducer. *Semin Nephrol* 25: 343–351, 2005.

37. **Sharifi AM, Li JS, Endemann D, and Schiffrin EL.** Effects of enalapril and amlodipine on small-artery structure and composition, and on endothelial dysfunction in spontaneously hypertensive rats. *J Hypertens* 16: 457–466, 1998.

38. **Wong LC and Langille BL.** Developmental remodeling of the internal elastic lamina of rabbit arteries: effect of blood flow. *Circ Res* 78: 799–805, 1996.

39. **Xavier FE, Rossoni LV, Alonso MJ, Balfagón G, Vassallo DV, and Salaices M.** Ouabain-induced hypertension alters the participation of endothelial factors in alpha-adrenergic responses differently in rat resistance and conductance mesenteric arteries. *Br J Pharmacol* 143: 215–225, 2004.

40. **Zhang J and Leenen FHH.** AT_1 receptor blockers prevent sympathetic hyperactivity and hypertension by chronic ouabain and hypertonic saline. *Am J Physiol Heart Circ Physiol* 280: H1318–H1323, 2001.